Membrane Technology
ISSN (online): 1873-4049

Vulnerability Analysis of Power System Considering the Multi-Scenario of Renewable Energy Output

Erwen HE[1], Shijun CHEN[2], Minghai XU[3*], Mengxiang DING[3], Yuqi HAN[1], Shengyong YE[1], Longjiang LI[4], Chenggang HE[4]

[1] *State Grid Sichuan Economic Research Institute, Chengdu, Sichuan Province, China.*

[2]*State Grid Sichuan Electric Power Company, Chengdu, Sichuan Province, China.*

[3] *School of Electrical Engineering, Southwest Jiaotong University, Chengdu, Sichuan Province, China.*

[4] *State Grid Ganzi Electric Power Supply Company, Ganzi, Sichuan Province, China.*

[*]*Correspondence: 1286389446@qq.com*

Abstract: *With the wind power penetration rising in recent years, the high uncertainty of the wind power increases the vulnerability and outage risk of power systems. In view of this, we propose a vulnerability analysis method considering the topology and state of the wind power grid-connected system. Firstly, we construct a wind power prediction model named as the Kmeans_HPO_GRU_LSTM model. Secondly, we propose a vulnerability evaluation method of the wind power grid-connected system based on the resilience betweenness of power flow considering the uncertainty of the wind power. Finally, the effectiveness and accuracy of the proposed method are verified by the simulations on the IEEE-39 bus system and a regional power grid in China, respectively.*

Keywords: *vulnerability, wind power prediction, resilience betweenness of power flow, wind power grid-connected system*

1 INTRODUCTION

Today, the whole world is undergoing green and low-carbon transformation, and developing and utilizing clean energy such as wind energy vigorously after the signing of the Paris Agreement. Clean power generation with the help of the wind power technology can help carbon peak and carbon neutrality, which is conducive to accelerating the construction of a clean and low-carbon energy system [1]. Affected by the natural conditions, wind power has uncontrollable random volatility, which will lead to the cascading trip-off of the wind turbines in centralized grid connection areas, and then increase the outage risk of power systems [2,3]. In 2016, the power grid in South Australia was affected by the extreme weather, which led to a chain reaction of the large-scale disconnection of the wind turbines and the faults of transmission lines, and then induced a major blackout [2]. In the power grid of London in 2019, a large number of wind turbines were disconnected due to the low frequency tolerance shortcomings of the wind turbines, and finally a large blackout occurred due to the large-scale power gap of the power grid [3]. Research showed that the high uncertainty of the wind power was an important factor to induce the vulnerability of the grid-connected system and increase the risk of the blackout. Therefore, it is of great significance to prevent blackouts by means of the effective and accurate vulnerability assessment of the wind power grid-connected system.

Power system vulnerability refers to the potential risks of the catastrophic cascades under the stochastic disturbances or faults [4]. Currently, the investigations into the vulnerability can be roughly divided into two aspects. The first focuses on the power flow and dynamic characteristics of the power system. It mainly includes transient stability analysis, brittleness theory, entropy theory, cascading fault simulation, risk assessment, energy function, reinforcement learning

and so on. Xia Y H et al. proposed a nonlinear decoupling method to evaluate the transient stability of the DC microgrid, which approximately transformed the nonlinear system into a low-order quadratic decoupling system [5]. He XF et al. put forward a novel vulnerability assessment method based on the branch fault state transition correlation, which accurately identified the vulnerable branches in the power grid [6]. Cao S proposed to use the power flow transfer entropy as a criterion to evaluate its transfer characteristics of the multi terminal direct current wind power grid-connected system [7]. Wu J considered the operation mechanism of the complex transmission network and potential cascade faults triggered in the recovery process and introduced the sequential recovery graph to identify the critical nodes and their recovery order [8].

Rocchetta R et al. proposed a power grid risk assessment model based on the line outage distribution coefficient to assess the severity of the cascades [9]. Fan WL et al. proposed a vulnerability assessment method of the high-speed rail grid-connected system based on the branch potential energy transfer entropy [10].

To evaluate and reduce the security risk of the deep reinforcement learning model in the power system, Zheng Y proposed a vulnerability evaluation method considering the noise data and the network attacks [11]. The other field concentrates the network structure mainly exploiting the complex network theory. It chiefly includes the improved betweenness method, maximum flow theory and dual graph method, etc. He. et al. the electrical energy resilience of microgrids operating in an islanded model under 72 hours of power interruption is verified by several metrics [12]. Zang T et al. proposed an identification method of key branches in the power grid based on the improved electrical betweenness by using the adjacency graph [13]. Considering the problem of the network vertex weight, Fang J et al. proposed an improved maximum flow method to evaluate the vulnerability of the power system [14]. Ege Kandemir discussed the predictive digital twin platform for wind energy systems in terms of data sources, modeling, and algorithms [15]. Fan WL et al. proposed a key line identification method based on the cascading failure state transition graph by using a modified H-index method [16].

The cited above only considers the power system vulnerability under a certain operating duty, and lacks the comprehensive vulnerability evaluation of the transmission lines under the influence of the wind power fluctuations. In view of this, we propose a vulnerability evaluation method of wind power grid-connected system based on the resilience betweenness of the power flow. In order to construct a high-precision wind power prediction model, firstly, we use the HPO optimization algorithm to realize the hyper-parameter optimization of the GRU_LSTM model, and combine with the Kmeans clustering method for the preprocessing of the input data. And then, develop a resilience betweenness of the power flow index that integrates the fluctuations of the wind power and state variables, and then construct a vulnerability evaluation model based on the resilience betweenness of the power flow.

The rest of the paper is arranged as follows. Section II introduces the framework and implementation process of wind power prediction which is based on a Kmeans_HPO_GRU_LSTM model. Section III proposes a vulnerability evaluation method of the wind power grid-connected system on the resilience betweenness of power flow. Section IV takes the IEEE-39 bus system and a regional power grid in China as examples to analyze and discuss the effectiveness and accuracy of the proposed method. Finally, a summary and some conclusions are drawn in Section VI.

2. Wind power prediction model

References [17] take advantage of the LSTM model has a large advantage in dealing with long sequence data, based on the LSTM model, update the model capacity, establish the online LSTM learning model architecture to realize the prediction of wind power, the computational formula is as Eq. (1), but it does not solve the problems of complex structure, high cost and so on. To overcome the above problems, reference [18] constructs wind power prediction model based on GRU model and superimposes the sub-prediction results to get the final prediction results, which is calculated as Eq. (2). However, it does not hide the disadvantages such as poorer memory capacity and higher quality requirements for data. References [19] combined the memory ability of GRU model and the ability of LSTM to deal with long-term dependencies, and established the GRU_LSTM model, which extracts the local and temporal features of the data, and then fuses the data features to perform wind power prediction using gating units. The model can deal with more structural types of data and has a more powerful ability to deal with unknown data, but the parameter settings of the model still limit the prediction accuracy.

Literature [17] constructed a wind power prediction model based on the capacity update of LSTM model, and the calculation formula is shown in equation (1), but the model did not solve the problems of complex structure and high cost. Literature [18] constructs a wind power prediction model based on GRU model, and the calculation formula is shown in Equation (2), but it still can't cover the disadvantages of poor memory capacity and high-quality requirements for data. For this reason, literature [19] combined the memory ability of GRU model and the ability of LSTM to deal with long-term dependencies. Then we build a wind power prediction model based on GRU_LSTM, but the parameter settings of this model still limit the prediction accuracy.

$$\begin{cases} f_t = \sigma(W_{fx}x_t + W_{fh}h_{t-1} + b_f) \\ i_t = \sigma(W_{ix}x_t + W_{ih}h_{t-1} + b_i) \\ g_t = \tanh(W_{gx}x_t + W_{gh}h_{t-1} + b_g) \\ O_t = \sigma(W_{ox}x_t + W_{oh}h_{t-1} + b_o) \\ C_t = g_t i_t + C_{t-1} f_t \\ h_t = \tanh(C_t) O_t \end{cases} \quad (1)$$

where σ is the sigmoid function, W is the weight matrix, b is the bias, h_{t-1} is the hidden state of the previous time, x_t is the input of the current time, C_{t-1} and are the memory units of the previous time and the current time respectively. The outputs of the input gate and the forgetting gate and the output gate are i_t and f_t and O_t, respectively.

$$\begin{cases} r_t = \sigma(W_t \cdot [h_{t-1}, x_t]) \\ z_t = \sigma(W_z \cdot [h_{t-1}, x_t]) \\ \tilde{h}_t = \Phi(W_{\tilde{h}} \cdot [r_t \times \mathrm{h}_{t-1}, x_t]) \\ h_t = (I - z_t) \times h_{t-1} + z_t \times \tilde{h}_t \\ y_t = \sigma(W_o \cdot h_t) \end{cases} \tag{2}$$

where y_t is the output at the current moment. h_t is the hidden state at the current time. r_t, z_t, $\tilde{h}_t$ are the state of update gate, reset gate and the current candidate set respectively. W_t, W_z, W_h, W_o are the weight matrix. Φ denotes the tanh activation function.

The above model accuracy problem shows the necessity of optimization algorithms in model hyperparameter optimization. In view of this, considering the better global optimization seeking ability and faster convergence speed of HPO optimization algorithm, this paper introduces Hunter-Prey- Optimizer (HPO) [4] for optimizing the hyperparameters of the GRU_LSTM model, which is computed as shown in Eq. 3 [20].

$$\begin{cases} x_i(\mathrm{t}+1) = T_{pos} + CZ\cos(2\pi R_4) \times (T_{pos} - x_i(t)), & R_5 > 0.1 \\ x_i(t+1) = x_i(t) + 0.5[(2CZP_{pos} - x_i(t)) + (2(1-C)Z\mu - X_i(t))], & R_5 < 0.1 \end{cases}$$

(3)

where $x(t)$ represents the current position of the prey, $x(t+1)$ is the next possible position of the prey, T is the global best position, R_5 represents a random number taken from it, C decreases from 1 to 0.02, Z is an adaptive parameter of the algorithm, and μ is the average of all positions.

Further, to address the problem that wind power prediction is affected by wind speed and direction, this paper utilizes the Kmeans method for high-dimensional classification of wind power data and explores the internal features of the data in order to improve the accuracy of prediction. In summary, the flow of the wind power prediction model based on Kmeans_HPO_GRU_LSTM is shown in Fig. 1.

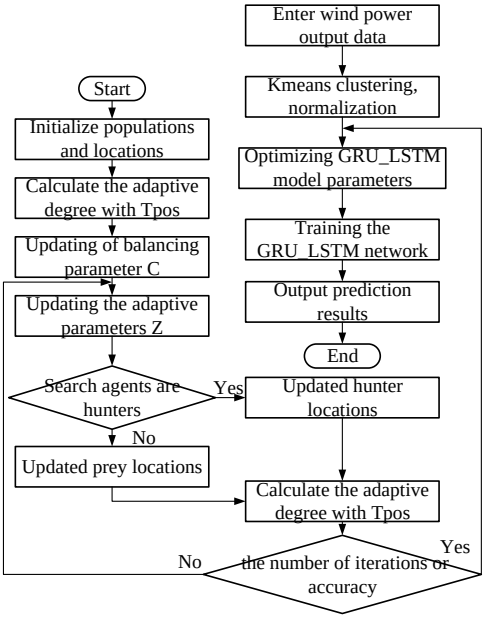

Figure.1 Flowchart of Kmeans_HPO_GRU_LSTM prediction model

The specific steps are as follows:

1) Normalize the historical wind power output data to avoid the influence of too large or too small range of values of certain features when training.

2) Define the degree of adaptation and take the average absolute error between the historical data and the predicted value of the GRU_LSTM network as the objective function of the HPO algorithm.

3) Use Kmeans clustering algorithm to perform high-dimensional clustering analysis of the data to obtain the m-class training set.

4) Use HPO algorithm to optimize the hyperparameters of GRU_LSTM model.

5) Construct the GRU_LSTM wind power output prediction model and train the m-class training set for model prediction respectively.

6) Use the parameter-optimized Kmeans_HPO_GRU_LSTM model for wind power prediction.

3. Vulnerability evaluation method of wind power grid-connected system

3.1 Resilience betweenness of power flow

3.1.1 Topological betweenness

According to the complex network theory, the betweenness of edge e is the ratio of the number of the shortest paths between any two nodes to the total number of the shortest paths [21], as shown in Eq. (4).

$$B_e = \sum_{i,j \in V} \frac{n_{ij(e)}}{n_{ij}} \tag{4}$$

where B_e is the betweenness of edge e. $n_{ij(e)}$ is the number of the shortest path between nodes i and j passes through edge e. n_{ij} represents the total number of the shortest paths between nodes i and j.

Edge or line betweenness is often used to measure the importance of the edge or line. The greater the edge or line betweenness, the greater the controllability of the edge / line in the network. Ref. [22,23] used the branch betweenness to reflect its criticality. However, the pure topology ignores the actual physical properties and conditional constraints of the power grid and cannot reflect the operation characteristics of the power grid. Ref. [22,24,25] put forward the concept of the weighted betweenness successively, which used the path with the lowest reactance as the shortest path to determine the vulnerable lines. Even so, they still fail to overcome the disadvantage that the power transmission is realized according to the principle of shortest distance and ignore the constraints of Kirchhoff's law in the power grid. According to the characteristics of the power flow transmission, Ref. [26] defined the electrical betweenness of the transmission lines, in which the unit current element was injected between the generator and the load nodes, and then the current would be generated on all lines. However, in the actual power system, only some lines are responsible for the power transmission between sources and sinks. Therefore, Ref. [27] proposed the concept of the power flow betweenness, which avoided the disadvantage that all lines carried the transmission power. However, it fails to consider the line transmission capacity and the electrical distance between the source and sink.

3.1.2 Resilience betweenness of power flow

Considering the disadvantages of the topological betweenness mentioned above, we propose the concept of the resilience betweenness of power flow. Since it considers the fluctuations of the wind power, the power constraints of the transmission lines and source-sink, which is more in line with the operation characteristics. We use it to identify the key lines in this paper.

Firstly, take the electric power and energy balance between the source and the sink and the constraints of the line power transmission capacity into account, and that is

$$P_{ijk} = \min(P_{ijk1}, P_{ijk2}) \tag{5}$$

$$P_{ijk1} = \min(P_i, P_j) \tag{6}$$

$$P_{ijk2} = \min\left(\frac{P_{l\max}}{PTDF_{ij}(l)} \mid l \in (1, 2, 3...n)\right) \tag{7}$$

where P_i, P_j represent the active power of the source i and the sink j respectively, $P_{l\max}$ is the maximum active power of transmission line l, and $PTDF_{ij}(l)$ is the power transmission distribution factor of the line l under the source i and the sink j. P_{ijk1} is the minimum value of the active power injected into the source i and the sink j, and P_{ijk2} is the minimum value of the power transmission of all lines under the source i and the sink j.

Eq. (5) introduces the power parameters to restrict the power balance. That is, the power of the source-sink will not exceed these limits, so as to ensure that the source-sink is in the balance of the supply and demand. Further, the carrying power of the transmission lines is guaranteed not to exceed the limits. To sum up, Eq. (5) considers the influences of the different generation capacities, load levels and the role of the line in the power transmissions on the importance of the lines.

Secondly, the wind power introduces the uncertainty into the system, resulting in the real-time fluctuation of the power flow with the wind power. In light of this, the previous vulnerability analysis based on the power flow under a certain operating duty needs to be improved. Therefore, considering the fluctuation of the wind power, we make the probability density function $P_{rk}(l)$ of active power of transmission line under probabilistic flow model[28] be incorporated in the vulnerability index to reflect the power fluctuations.

In general, the power constraints of the same line under different source-sink pairs are different, and its PTDFs are also different. When using the Monte Carlo algorithm to calculate the probabilistic flows, we get the cumulative probability distribution after multiple sampling. And then we can get the resilience betweenness of power flow index, and that is

$$B_l = \sum_{i\in G}\sum_{j\in L}\sum_{k=1}^{N} P_{ijk} \times P_{rk}(l) \tag{8}$$

where G is the set of the sources, and L is the set of the sinks. N is the number of the Monte Carlo calculations.

The resilience betweenness of power flow reflects the relative importance of the transmission lines under the view of the topology and operation state for the wind power grid-connected system. In addition, considering the number of the source-sink pairs and the calculation times of the probabilistic power flow, it can reflect the span of the line utilized. At the same time, considering the generation capacity and load level and the power constraint of transmission lines, it can reflect the actual operation state and margin of the line, and show the depth of the line exploited.

3.2 Esilience betweenness of power flow

3.2.1 Vulnerability evaluation model

The vulnerability evaluation model of wind power grid-connected system in Figure 2.

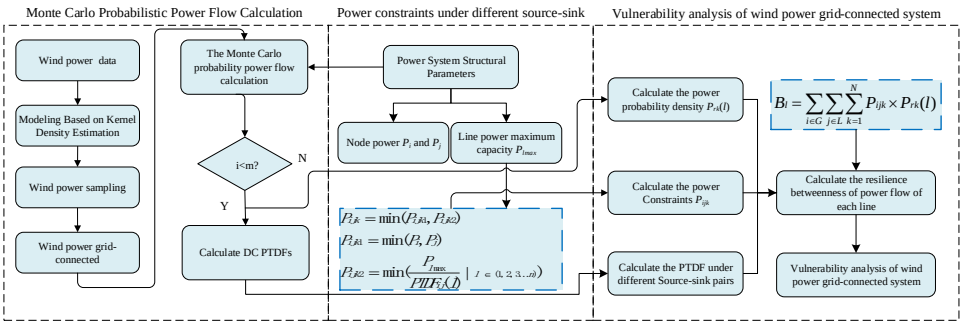

Figure 2. Vulnerability analysis model of wind power grid-connected system

The specific steps are as follows.

Step 1. According to the historical data of the wind power, we establish the probability model of the wind power by using the nonparametric kernel density estimation method. The established probability model is sampled by latin hypercube sampling to obtain the large samples of the power flows. Finally, the wind power scenarios are extracted according to the K-means clustering method.

Step 2. According to the sampling data in different scenarios, we calculate the Monte Carlo probability flows of N times, and obtain the probability density of the power of all transmission lines.

Step 3. Calculate the power constraints of transmission lines under different source-sink pairs according to Eq. (5).

Step 4. Calculate the resilience betweenness of power flow of each line according to Eq. (8) and identify the vulnerability of the wind power grid-connected system.

3.2.2 Verification indices

The outages of the power system are often caused by the cascades, which will lead to the collapse of the system finally. Among them, a very few critical lines play an important role in the power system faults. Therefore, we can evaluate the vulnerability according to the consequences of cascades after the line faults, and then identify the vulnerable lines [29]. Generally, the changes of the network performance after the line trip-off is used to measure and judge its importance. In this paper, we will adopt two indices, and that are the load loss rate [30] and net-ability [31] respectively.

a. Load loss rate

We choose the static attack mode for cascading failure simulations in this paper and cut off the corresponding lines according to the descending order of the resilience betweenness of power flow. Calculate the average load loss triggered by each line [30] according to Eq. (9). The greater the value of $P_{loss}(i)$, the more vulnerable the line is.

$$P_{loss}(i) = \frac{\sum_{n=1}^{R} ploss(n)}{R} \tag{9}$$

where $P_{loss}(i)$ and $ploss(n)$ refer to the average load loss and the load loss after line i is disconnected respectively, and R is the simulation times.

b. Net-ability

The Net-ability measures the power supply capacity of the power grid from the structural level, which is limited by both the line transmission capacity and line equivalent impedance [31], as shown in Eq. (10).

$$A_Y = \frac{1}{N_G N_D} \sum_{g \in G} \sum_{d(d \neq g) \in D} C_g^d \frac{1}{\left| Z_g^d \right|} \tag{10}$$

4. Case study

4.1 Wind power output forecast results

The GRU_LSTM model, HBA_GRU_LSTM model, WOA_GRU_LSTM model, HPO_GRU_LSTM model, and the Kmeans_HPO_GRU_LSTM model were used for wind power prediction, respectively, and the mean absolute error (MAE), the root-mean-square error (RMSE), and the symmetric mean absolute percentage error (SMAPE) as quantitative indicators to facilitate the comparison of the prediction results of multiple models, and the smaller the value of these three data sets, the better the prediction effect is proved. The results are shown in Figure 3.

It can be clearly seen from Fig. 3 that the original GRU_LSTM prediction model has a great error, and in the test set, the RMSE, MAE, and SMAPE reach 4.139, 3.913, and 0.315, respectively, whereas the prediction accuracy of the model with parameter optimization, especially the model optimized by the chosen HPO algorithm, is greatly improved, and in the test set, the RMSE, MAE, and SMAPE are 0.7, 0.538, and 0.035, respectively, much smaller than those of the original prediction model and other optimization algorithms, and can predict wind power output much more effectively, SMAPE are 0.752, 0.538 and 0.042 respectively, which are much smaller than the original prediction model and the prediction models of other optimization algorithms, and can predict the wind power output more effectively.

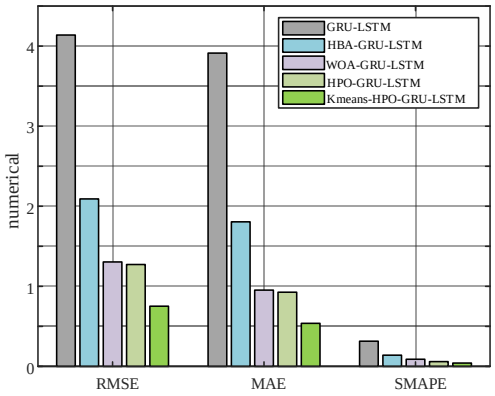

Figure3. Indicators for evaluating the results of different model predictions

4.2 IEEE 39 Bus system

The system is a New England transmission network, which consists of 39 nodes, 46 branches and 10 generators. The topology of the system is shown in Figure 4.

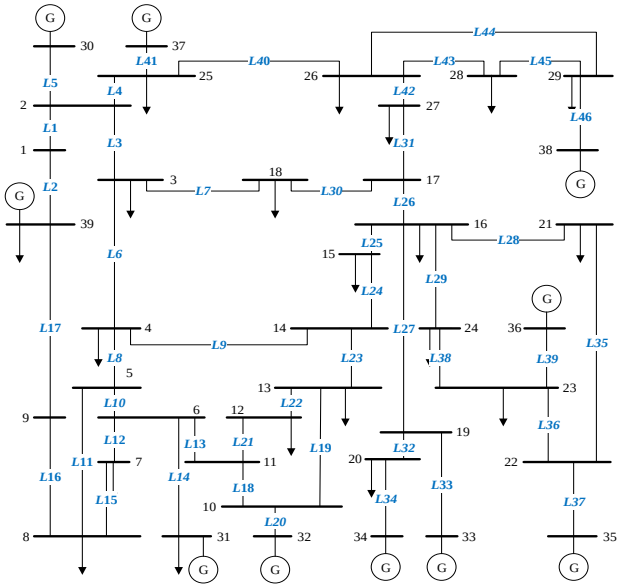

Figure 4. IEEE-39 Bus System

We sort the resilience betweenness of power flow of the transmission lines in descending order in Figure 5. Among them, the first 6 vulnerable lines are shown in Table 1.

Table 1 Resilience betweenness of power flow of the top 6 vulnerable lines in the IEEE-39 bus system

sort	line number	connection bus	normalized value
1	5	2-30	1.0000
2	37	22-35	0.9714
3	20	10-32	0.9222
4	41	25-37	0.8445
5	46	29-38	0.8318
6	39	23-36	0.7463

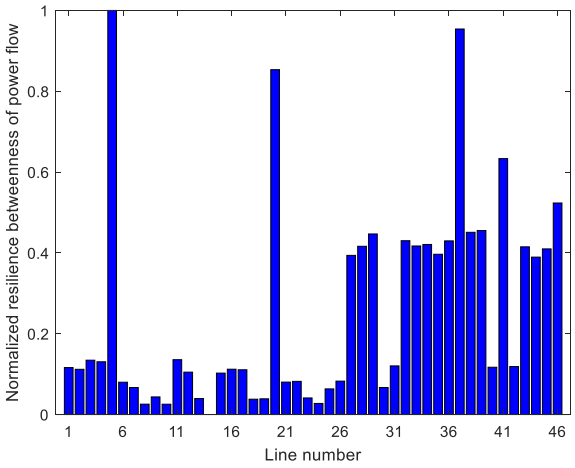

Figure 5. Vulnerable lines in the IEEE-39 Bus System

Figure 6 shows the ranking orders of the vulnerable lines under the resilience betweenness of power flow method (RBPF) method, the topological potential method (TPS) [32], the PageRank algorithm (PR) [33] and the maximum flow method (MF) [34] respectively. As we know, TPS method introduces the topological potential of the data field theory into the vulnerability analysis of the power system. PR method extends the concept of interaction graph and builds a directed weighted graph according the cascades. MF method is a new centrality measure based on the maximum flow between the source and the sink.

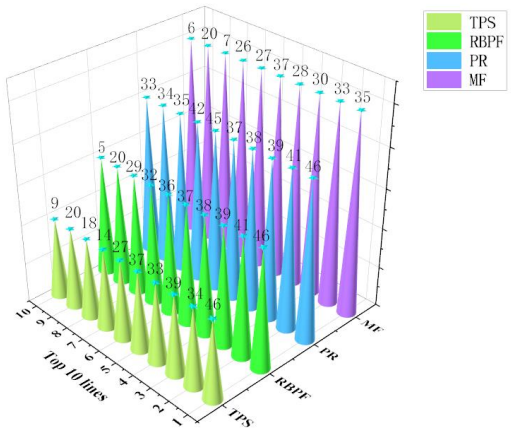

Figure 6. Comparison of different vulnerability identification results in the IEEE-39 bus system

From Figure 6, we can see that 5-10th of vulnerable lines identified by the RBPF method and PR method are the same, and 4-10th of the lines are the same for the RBPF method and TPS method, which verifies the effectiveness of the RBPF method. Besides, since the MF method only considers the branch overload among the faults, its effect to obtain the vulnerable lines is the worst. Further, in order to verify the accuracy of the RBPF method, we deliberately attack the top 6 vulnerable lines identified by the different methods, as shown in Figure 7. Figure 7 (a) shows that the remaining load rate of the system is 92.16% after attacking the top 6 vulnerable lines under the MF method, which shows that the removals of the vulnerable lines have little impact on the system, so the identification effect of the MF method is the worst. But the remaining load rates under the PR method, the TPS method and the RBPF method are 65.1%, 52.6% and 46.46% respectively. So clearly, the load loss corresponding to the RBPF method is the most serious. Thus, it can be seen that the vulnerable lines identified by the RBPF method have the best effect.

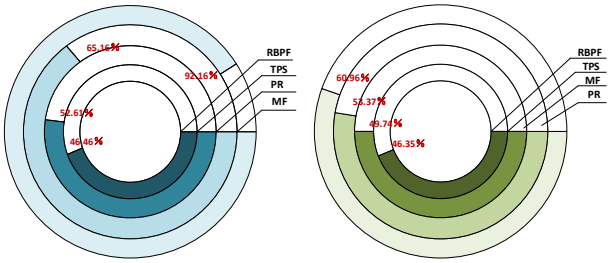

(a) Residual load rate **(b)** Net-ability

Figure 7. Network performance changes under different removal strategies in the IEEE-39 bus system

As can be seen from Figure 7 (b), the net-ability is the lowest, only 46.35% after removing the top 6 vulnerable lines under the RBPF method, compared to 49.74% and 60.96% under the TPS method and the PR method respectively. Therefore, it can be concluded that the outage risk is closely related to the vulnerable lines. The higher the vulnerability of the lines, the greater the outage risk.

Next, we will compare and analyze the changes of the vulnerability under the typical scenarios of the wind power, as shown in Figure 8.

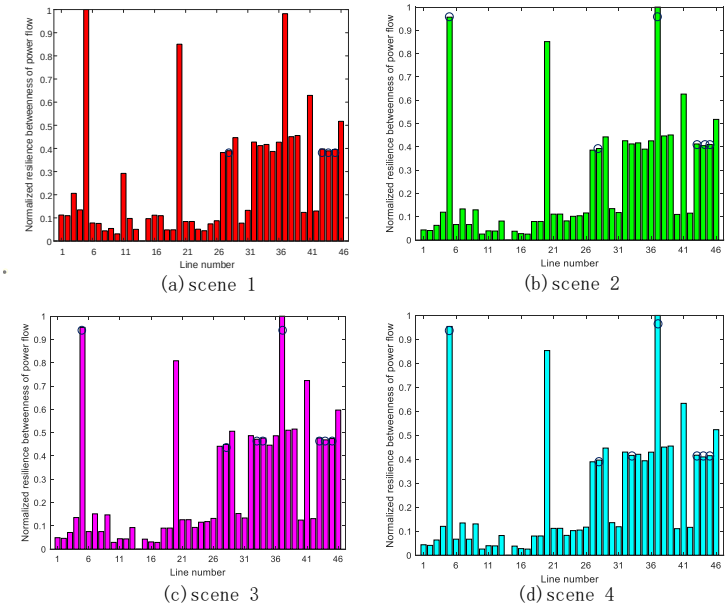

Figure 8. Identification of vulnerable lines in different scenarios

As can be seen from Figure 8, the ranking orders of the vulnerable lines obtained in different scenarios are different. Compared with the top 16 vulnerable lines in non-scenario, there are 4 different vulnerable line order in the first scenario. The corresponding values in the other scenarios are 6, 8 and 7 respectively. In order to further analyze the impact of the different scenarios on the vulnerability, we deliberately attack the vulnerable lines in different scenarios, and then analyze the sections where the remaining load rate and net-ability change the most, as shown in Figure 9.

As can be seen from Figure 9 (a), the remaining load rates of the system under different scenarios have changed significantly from the attacks on the 11th line. The biggest changes correspond to the first scenario, the second scenario and fourth scenario. The final remaining load rate is 23.67%, which shows that these scenarios have the greatest impacts on the power grid and have higher possibilities of the outages. In the third scenario, the final remaining load rate is 24.68% after attacking the first 16 vulnerable lines. In addition, the wind power of the non-scenario has the least impact on the power grid, and the remaining load rate is 25.25%. Therefore, different typical scenarios should be considered when connecting the wind farm to the power grid, and the power grid shall be protected for different typical scenarios. While in Figure 9 (b), we can find that different scenarios have different impacts on the vulnerability. In the initial stage, the net-ability

changes fastest in non-scenario, the first scenario and the second scenario, followed by the fourth scenario and the third scenario. After attacking the first 16 lines, the net-abilities in the non-scenario and the first scenario are only 22.26%, while those of the other scenarios are the same, which are 22.59%.

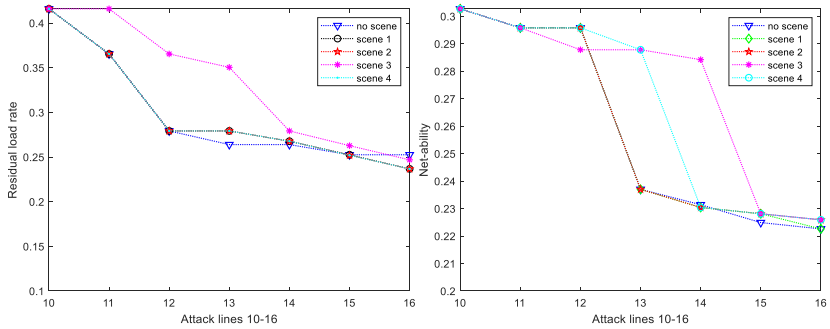

(a)Lines 10-16 Residual load rate (b)Lines 10-16 Net-ability

Figure 9. Network performance Changes for attacking the top 10th-16th vulnerable lines in the IEEE-39 bus system

As we know, different grid-connected points of the wind farm will cause various changes of power flow. We connect the wind farm to nodes 9, 19, 35 and 38, and the vulnerable lines are shown in Figure 10.

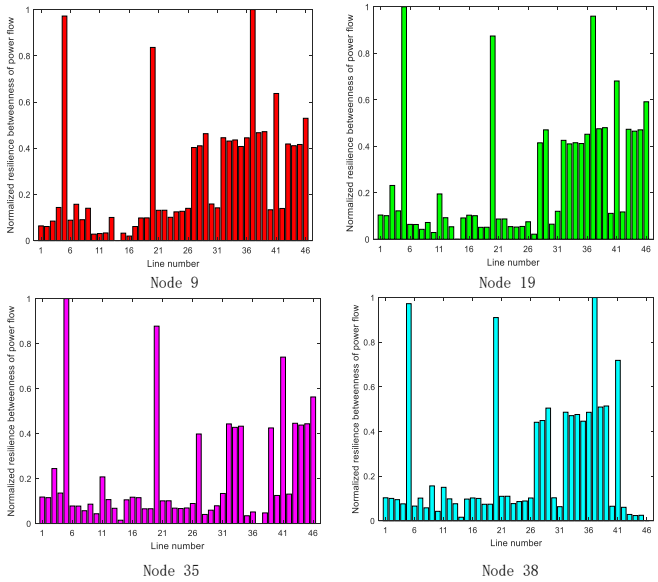

Figure 10. Vulnerable lines under different wind power grid-connected points in the IEEE-39 bus system

It can be seen from Figure 10 that different grid-connected points of the wind farm have different effects on the vulnerability. To further analyze the effects, we deliberately attack the vulnerable lines under different grid-connected points. Figure 11 shows the section with the largest change in the remaining load rate and the net-ability.

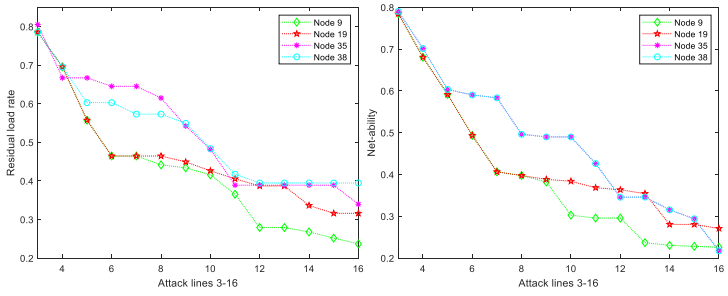

(a)Lines 3-16 Residual load rate (b)Lines 3-16 Net-ability

Figure 11. Network performance changes for attacking the top 3rd-16th vulnerable lines in the IEEE-39 bus system

As can be seen from Figure 11 (a), when we attack the first 16 lines, the wind farm connected to the node 9 has the greatest impact on the vulnerability, and the remaining load rate is 23.67%, which is most likely to cause a major outage. The remaining load rates when we connect the wind power to nodes 19 and 35 are 31.61% and 33.97% respectively. The connection of node 38 has a relatively small impact on the system, and the remaining load rate is 39.47%. As can be seen from Figure 11 (b), the system is most affected when the wind farm is connected with node 9, while selecting nodes 35 and 38 has the least impact on the vulnerability. Therefore, node 9 is not conducive to connect the wind farms.

4.3 NE power system in China

In this section, we take a regional power grid in China as an example to verify the effectiveness and accuracy of the RBPF method. The system has 32 nodes, 42 branches and 9 generators. For convenience, the system is recorded as NE system, as shown in Figure 12.

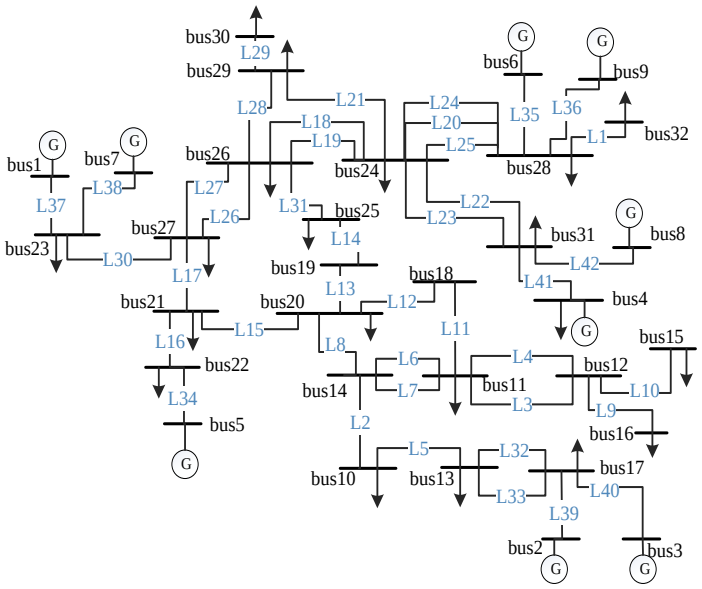

Figure 12. The NE power system

We analyze the vulnerability of the NE network and the results are shown in Table 2.

Table 2 Resilience betweenness of power flow in the NE power system

sort	line	RBPF	sort	line	RBPF	sort	line	RBPF
1	39	1.000	15	23	0.455	29	6	0.259
2	40	0.995	16	5	0.449	30	7	0.258
3	41	0.990	17	30	0.418	31	11	0.252
4	42	0.988	18	28	0.301	32	12	0.251
5	36	0.898	19	26	0.300	33	8	0.248
6	37	0.879	20	27	0.299	34	2	0.237
7	38	0.873	21	21	0.281	35	24	0.232
8	34	0.786	22	31	0.279	36	25	0.229
9	1	0.642	23	17	0.277	37	20	0.227
10	29	0.563	24	15	0.276	38	35	0.154
11	32	0.537	25	18	0.271	39	10	0.059
12	33	0.532	26	19	0.270	40	9	0.052
13	16	0.498	27	13	0.269	41	3	0.013
14	22	0.457	28	14	0.268	42	4	0.000

Further, in order to verify the accuracy of the RBPF method, we deliberately attack the first 6 vulnerable lines under different methods, as shown in Figure 13.

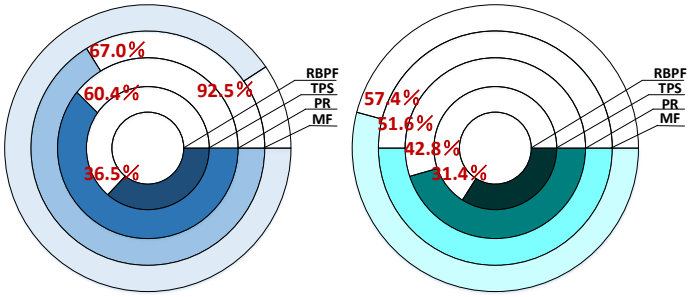

(a) Residual load rate **(b)** Net-ability

Figure 13. Network performance under different attacking methods in the NE power system

As can be seen from Figure 13 (a), the RBPF method has the best effect. The remaining load rate of the system is 36.5% after removing the vulnerable lines, indicating that these vulnerable lines have a great impact on the vulnerability. Correspondingly, they are 60.4%, 67% and 92.5% under the TPS method, the PR method and MF method, respectively. The same conclusion can be obtained from Figure 13 (b). From the above comparative analysis, we can see that the RBPF method can better identify the vulnerable lines, which reflects the advantages of this method. Figure 14 shows the vulnerable lines after we connect the wind farm to nodes 2, 5, 8 and 13 respectively in the NE network.

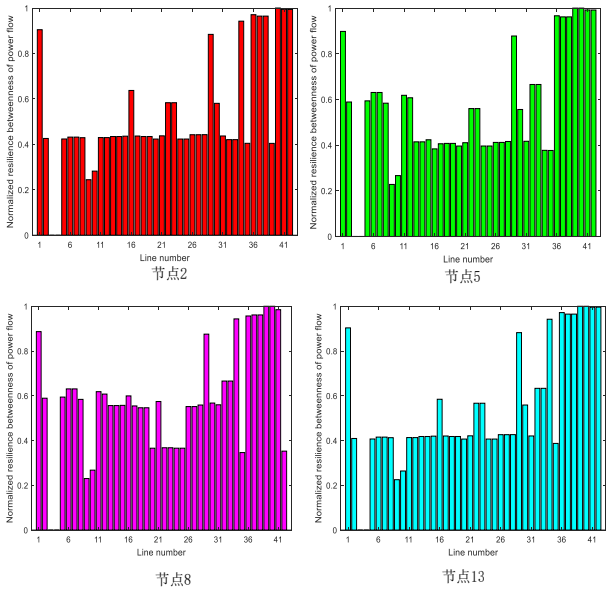

Figure 14. Vulnerable lines when wind power is connected to different nodes in the NE power system

It can be seen clearly from Figure 14 that the vulnerable lines obtained vary with the different grid-connected points. Next, we will still attack the first 16 vulnerable lines and analyze the changes of the remaining load rate and net-ability, as shown in Figure 15.

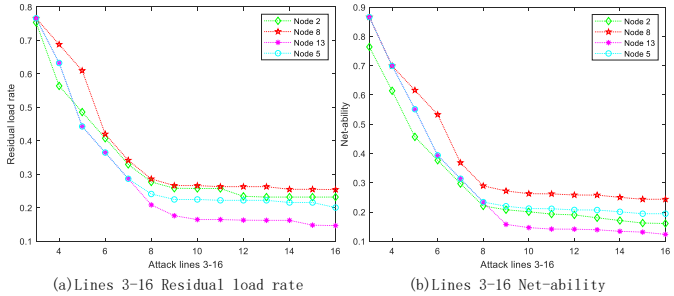

Figure 15. Network performance changes for attacking the 3rd to the 16th vulnerable lines in the NE power system

As can be seen from Figure 15 (a) and (b), the remaining load rate is 14.66% and the net-ability is 12.35% when the wind farm is connected to node 13. At this time, the wind farm has the greatest impact on the system and is very easy to induce a blackout. In addition, the system is the least affected when the wind farm is connected to node 8, because the remaining load rate is 25.43% and the net-ability is 24.36%. In view of this, node 13 is not conducive to be connected to the wind farm in the NE power grid.

5. Summary

Vulnerable line identification is an important aspect of the vulnerability analysis of the complex power grid. Considering the fluctuations of the wind power and the changes of the power flows, we have proposed a vulnerability evaluation method of the wind power grid-connected system based on the resilience betweenness of power flows taking the structure and operation state into account. Through the simulations on the IEEE-39 bus system and an actual power grid in China, we have known that the identification accuracy of the proposed RBPF method is higher than that of the TPS, MF and PR methods. In addition, according to the method proposed in this paper, the impacts of different nodes connected to the wind farm on the vulnerability will be conducive to the grid-connected planning of the wind farm.

Funding

This work was supported by Science and Technology Project of State Grid Sichuan Electric Power Company under Grant B7199624M002(Research on Key Technologies of "Grid-forming Energy Storage + Renewable Energy" Supporting Weak Link Power Grids by State Grid Sichuan Economic Research Institute in 2024, B7199624M002).

REFRENCES

[1] WANG Z Y, WU D H, WANG Y, et al. Stochastic gradient identification algorithn for nonlonear system modeling in wind power curtailment prediction. Modern Physics Letter B 2017 31:19-21.
[2] Yan RF, Nahid AM, Saha TK Bai FF, Gu HJ. The Anatomy of the 2016 South Australia Blackout: A Catastrophic Event in a High Renewable Network. IEEE Transactions on Power Systems 2018;33(5): 5374-88.
[3] Sun H, Xu T, Guo Q, Li Y, Lin W, Yi J,et al. Analysis on Blackout in Great Britain Power Grid on August 9th, 2019 and Its Enlightenment to Power Grid in China. Proceedings of the Chinese Society of Electrical Engineering 2019;39(21): 6183-92.
[4] Fouad AA, Zhou Q, System vulnerability as a concept to assess power system dynamic security. IEEE Transactions on Power Systems 1994;9(2):1009-15.
[5] Xia Y , Wei W, Long T, Blaabjerg F, Wang P. New Analysis Framework for Transient Stability Evaluation of DC Microgrids. IEEE Transactions on Smart Grid 2020; 11(4): 2794-804.
[6] He X F, Fan W L. Vulnerability assessment of power system based on Theil entropy of branch potential energy[J]. Physica Scripta 2021;96(4):045207
[7] Cao S, Zhang X, Xiang W, Wen J. A Power Flow Transfer Entropy Based AC Fault Detection Method for the MTDC Wind Power Integration System. IEEE Transactions on Industrial Electronics 2021; 68(11): 11614-20.
[8] Wu J, Chen Z, Zhang Y, Xia Y, Chen X. Sequential Recovery of Complex Networks Suffering From Cascading Failure Blackouts. IEEE Transactions on Network Science and Engineering 2020;7(4): 2997-3007.
[9] Rocchetta R, Patelli E. A post-contingency power flow emulator for generalized probabilistic risks assessment of power grids. Reliability Engineering & System Safety 2020;197:106817.
[10] Fan W L, Xiao Y Q, He X F, Li Q Y, Hu P, Ye Y. Vulnerability of high-speed rail grid-connected system on branch potential energy transfer entropy. Physica Scripta 2021;96(12):125241.
[11] Zheng Y, Yan Z M, Chen K J,Sun J, Xu Y, Liu Y. Vulnerability Assessment of Deep Reinforcement Learning Models for Power System Topology Optimization. IEEE Transactions on Smart Grid 2021;12(4): 3613-23.
[12] Liu B, Li Z, Chen X, Huang Y, Liu X .Recognition and vulnerability analysis of key nodes in power grid based on complex network centrality. IEEE Transactions on Circuits and Systems II: Express Briefs 2018;65(3):346-50.
[13] Zang T L, Gao S B, Huang T, Wei X, Wang T. Complex network-based transmission network vulnerability assessment using adjacent graphs. IEEE Systems Journal 2020;14(1):572-81.
[14] Fang J, Su C, Chen Z, Sun H, Lund P. Power System Structural Vulnerability Assessment Based on an Improved Maximum Flow Approach. IEEE Transactions on Smart Grid 2018;9(2):777-85.
[15] Liu Y, Gao S, Shi J, Wei X, Han Z. Sequential-Mining-Based Vulnerable Branches Identification for the Transmission Network Under Continuous Load Redistribution Attacks. IEEE Transactions on Smart Grid 2020;11(6):5151-60.

[16] Fan W L, He X F, Xiao Y Q, et al. Vulnerability analysis of Power System by Modified H-index Method on Cascading Failure State Transition Graph[J]. Electric Power Systems Research, 2022, 209: 107986/1-8
[17] C. Pan, S. Wen, M. Zhu, H. Ye, J. Ma and S. Jiang, "Hedge Backpropagation Based Online LSTM Architecture for Ultra-Short-Term Wind Power Forecasting," in IEEE Transactions on Power Systems, vol. 39, no. 2, pp. 4179-4192, March 2024.
[18] Y. Cai, D. Wei and F. Zhou, "Research on short-term wind speed prediction based on EEMD-GRU prediction model," 2023 IEEE 3rd International Conference on Electronic Technology, Communication and Information (ICETCI), Changchun, China, 2023, pp. 647-651.
[19] DING X, PAN X P, HE D Z, et al. Wind farm dynamic equivalent modeling by GA-optimized GRU-LSTM-FC combined network[J]. Electric Power Automation Equipment, 2023,43(08):119-125.
[20] Naruei I, Keynia F, Molahosseini AS. Hunter-prey optimization: algorithm and applications[J]. Soft Computing, 2022, 26(3): 1279-1314.
[21] An B K, Feng Y. Complex network theory in the application of optimization topology network. 3rd International Conference on Advanced Engineering Materials and Architecture Science (ICAEMAS) 2014; 1811-5.
[22] Chen G, Dong Z, Hill DJ, Zhang G, et al. An improved model for structural vulnerability analysis of power networks. Physica a-Statistical Mechanics and Its Applications 2009; 388(19): 4259-66.
[23] Rosas-Casals M, Valverde S, Sole RV. Topological vulnerability of the European power grid under errors and attacks. International Journal of Bifurcation and Chaos 2007;17(7): 2465-75.
[24] Liu Y, Zhu X, Kang K, Lin Y, Yu J, Wang Y. Identification of vulnerable lines in power grid based on the weighted reactance betweenness index. Power System Protection and Control 2011;39(23): 88-92.
[25] Ding M, Han P. Vulnerability Assessment to Small-world Power Grid Based on Weighted Topological Model. Proceedings of the Chinese Society of Electrical Engineering 2008; 28(10): 20-5.
[26] Xu L, Wang X, Wang X. Cascading Failure Mechanism in Power Grid Based on Electric Betweenness and Active Defence. Proceedings of the Chinese Society of Electrical Engineering 2010;30(13): 61-8.
[27] Liu W, Liang C, Xu P , et al. Identification of critical line in power systems based on flow betweenness[J]. Proceedings of the Chinese Society of Electrical Engineering, 2013, 33(31):90-98.
[28] Nassar M E, Salama M A Novel Probabilistic Load Model and Probabilistic Power Flow. IEEE 28th Canadian Conference on Electrical and Computer Engineering (CCECE) 2015;881-886.
[29] Ding L, Liu M, Cao Y, Han Z. Power System Key-lines Identification Based on Hidden Failure Model and Risk Theory. Automation of Electric Power Systems 2007;31(6): 1-5.
[30] Ma Z Y, Liu F , Shen C, Zhang S, Tian B. Rapid Identification of Vulnerable Lines in Power Grid Using Modified PageRank AlgorithmPart I: Theoretical Foundation. Proceedings of the Chinese Society of Electrical Engineering 2016;36(23): 6363-70.
[31] Arianos S, Bompard E, Carbone A, Xue F, Power grid vulnerability: A complex network approach. Chaos 2009;19(1):013119.
[32] Fan W L, Li Q Y, Xiao Y Q, He X F, Tong Y Z, Hu P, et al. Power system vulnerability analysis based on topological potential field theory. Physica Scripta 2021; 96(12):125227.
[33] Ma Z, Shen C, Liu F, Mei S. Fast Screening of Vulnerable Transmission Lines in Power Grids: A PageRank-Based Approach. IEEE Transactions on Smart Grid 2019;10(2): 1982-91.
[34] Rocchetta R and Patelli E, Assessment of power grid vulnerabilities accounting forstochastic loads and model imprecision. International Journal of Electrical Power & Energy Systems 2018; 98: 219–32.